Back to Session Subjects

NONLINEAR PASSIVITY-BASED CONTROL FOR A SCALE MODEL HELICOPTER

Juan Carlos Avila Vilchis* Bernard Brogliato†

Laboratoire d'Automatique de Grenoble
ENSIEG, BP 46. UMR CNRS-INPG 5528
38402, Saint Martin D'Hères
France

Keywords: helicopter, nonlinear control, dissipativity, underactuated.

Abstract.

This work focuses on the nonlinear control of helicopters. A scale model helicopter (Benzin Trainer) of the University of Technology of Compiègne (France) will serve later for experiments. Our global interest is a general model (7-DOF) obtained to be used on the autonomous forward-flight of the helicopter. However, in this paper we present a reduced-order model (3-DOF) representing the helicopter mounted on an experimental platform. Although simplified, this 3-DOF Lagrangian model presents quite interesting control challenges due to nonlinearities, aerodynamical forces and underactuation. Due to the very particular dynamical and control properties of the model we propose a specific nonlinear controller using passivity properties. Numerical simulations are presented.

1. Introduction.

In this note we consider the problem of controlling a scale model helicopter when it is mounted on a platform. Though the mathematical model of this system is much simpler than that of the "free-flying" helicopter, its dynamics will be shown to be non-trivial (nonlinear in the state, and underactuated).

Contrary to most of the recent works in the field of nonlinear control of helicopters [1], [3] and [5], we incorporate the main and tail rotors dynamics in the Lagrange equations. Moreover the control inputs are taken as the real helicopter inputs (the translational displacements of the main and tail rotors collective pitches and the longitudinal and lateral cyclic pitch angles of the main rotor). This is shown to complicate significantly the way the input u appears in the Lagrange equations ($u \in \mathbb{R}^4$ for the 7-DOF model and $u \in \mathbb{R}^2$ for the 3-DOF model studied in this paper).

This paper is organized as follows. In section 2 we present a Lagrangian model of the helicopter mounted on an experimental platform. This model can be seen as made of two subsystems (translation and rotation). The dissipativity properties of the model are analyzed in section 3 where one lossless operator is shown. In section 4 we present a two steps control design (one step for each subsystem). Section 5 is devoted to simulation results. In section 6 we present some conclusions of this work. Finaly the values for the model parameters are given in appendix A.

2. Model of the Helicopter-Platform.

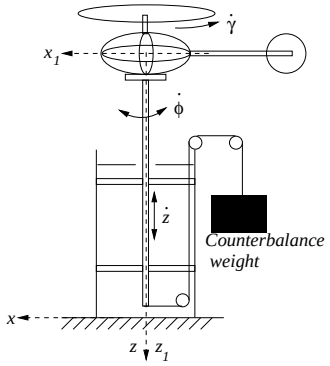

Figure 1: Platform.

We consider figure 1 where the counterbalance weight compensates the weight of the vertical column of the platform. The xyz reference system is an inertial one and the $x_1y_1z_1$ reference system is a body fixed frame. The model is obtained by a Lagrangian formulation. The kinetic energy T is formed by four quantities: T_t, T_{rf}, T_{rM} and T_{rT} corresponding to kinetic energy of translation and kinetic energy of rotation of the fuselage, the

*Juan-Carlos.Avila-Vilchis@inpg.fr
†Bernard.Brogliato@inpg.fr

main rotor and the tail rotor, respectively. The potential energy is formed by the gravitational potential energy U_g and by the flapping potential energy U_b. In the particular case that we present here, $U_b = 0$.

The model has the next form:

$$M(q)\ddot{q} + C(q,\dot{q})\dot{q} + G(q) = Q(u) \qquad (1)$$

where M is the 3×3 inertia matrix, C is the 3×3 Coriolis matrix, $G \in \mathbb{R}^3$ is the vector of conservative forces, $Q = [f_z \;\; \tau_z \;\; \tau_\gamma]^T$ is the vector of generalized forces, $q = [z \;\; \phi \;\; \gamma]^T$ is the vector of generalized coordinates and $u = [h_M \;\; h_T]^T$ is the vector of control inputs. h_M and h_T are the translational displacements of the main and tail rotors collective pitches respectively. They are proportional to the collective pitch angles of the main and tail rotors respectively. The height $z < 0$ upwards, ϕ is the yaw angle and γ is the azimuth angle of the main rotor blades.

The components of the vector Q are [4], [6]: $f_z = T_m + D_{vi}$, $\tau_z = T_T d$ and $\tau_\gamma = Q_M + Q_{mot}$. T_M is the thrust of the main rotor, D_{vi} is the drag force produced by the induced velocity, T_T is the thrust of the tail rotor, d is a known constant, Q_M is the drag moment of the main rotor and Q_{mot} is the moment of the engine.

The various terms in (1) are:

$$M(q) = \begin{bmatrix} c_0 & 0 & 0 \\ 0 & c_1 + c_2\cos^2(c_3\gamma) & c_4 \\ 0 & c_4 & c_5 \end{bmatrix}$$

$$C(q,\dot{q}) = \begin{bmatrix} 0 & 0 & 0 \\ 0 & c_6\sin(2c_3\gamma)\dot{\gamma} & c_6\sin(2c_3\gamma)\dot{\phi} \\ 0 & -c_6\sin(2c_3\gamma)\dot{\phi} & 0 \end{bmatrix}$$

$$G(q) = \begin{bmatrix} c_7 \\ 0 \\ 0 \end{bmatrix} \qquad (2)$$

with the assumption that the helicopter evolves at low rates of vertical velocity so that the vertical flight induced velocity and the hover induced velocity are approximately equal ($v_v \approx v_h$), taking $Q(u) = A(\dot{q})u + B(\dot{q})$ and from [4]

$$A(\dot{q}) = \begin{bmatrix} c_8\dot{\gamma}^2 & 0 \\ 0 & c_{11}\dot{\gamma}^2 \\ c_{12}\dot{\gamma} - c_{13} & 0 \end{bmatrix}$$

$$B(\dot{q}) = \begin{bmatrix} c_9\dot{\gamma} + c_{10} \\ 0 \\ c_{14}\dot{\gamma}^2 + c_{15} \end{bmatrix} \qquad (3)$$

where the c_i's $i = 0, ..., 15$ are constant physical parameters.

One sees that this model is made of two main coupled subsystems $S_{translation}$ and $S_{rotation}$ with states $(z, \dot{z})$ and $(\phi, \dot{\phi}, \gamma, \dot{\gamma})$ respectively. This will be used for control design.

3. Dissipativity Properties of the Model.

The use of passivity has been at the core of the design of many feedback controllers in the past fifteen years (see [2]). The interest of passivity-based controllers comes from their physical foundations (contrary to some other nonlinear stabilization techniques which rely only on the state-space equations structure). They also prove to provide nice experimental results [2].

The design of a passivity-based controller for (1) is however quite specific due to both the Lagrangian dynamics and the form of $Q(u)$. More precisely, the z dynamics in (1) plus the fact that the inputs in u are not generalized forces, precludes the dissipativity of the operators:

$$O_1 : u \mapsto \dot{q}$$
$$O_2 : Q(u) \mapsto \dot{q}$$

a property that is crucial in the design of passivity-based controllers which assure global tracking control of $(q(t), \dot{q}(t))$. However the operator:

$$O_3 : \bar{u} \triangleq \bar{A}u + \bar{B} \mapsto \dot{\eta} \triangleq [\dot{\phi} \;\; \dot{\gamma}]^T \qquad (4)$$

is passive lossless, with:

$$\bar{M} = \begin{bmatrix} m_{22} & m_{23} \\ m_{32} & m_{33} \end{bmatrix} \quad \bar{C} = \begin{bmatrix} c_{22} & c_{23} \\ c_{32} & 0 \end{bmatrix}$$
$$\bar{A} = \begin{bmatrix} 0 & a_{22} \\ a_{31} & 0 \end{bmatrix} \quad \bar{B} = \begin{bmatrix} 0 \\ b_3 \end{bmatrix} \qquad (5)$$

The proof is easy by noting that $\dot{\bar{M}} - 2\bar{C}$ is skew symmetric [2].

4. Control Design.

For feedback control purpose, we will use both the structure of the dynamics in (1)-(3), and the physical property of the operator $O_3 : \bar{u} \mapsto \dot{\eta}$.

In the following we assume that initially $|\dot{\gamma}(0)| \geq \delta > 0$ and $z(0) < 0$, so that $\bar{A}$ is full rank. The whole problem including take-off and landing will be treated for the 7-DOF model (taking ground-effects into account). Therefore the control design is done in two steps:

4.1. Passivity-based tracking control of the rotational part.

The rotational dynamics is given by (see (5)):

$$\bar{M}(\eta)\ddot{\eta} + \bar{C}(\eta,\dot{\eta})\dot{\eta} = \bar{A}(\dot{\eta})u + \bar{B}(\dot{\eta}) \qquad (6)$$

It is note worthy that this dynamics also represents the rotational part of the system when the helicopter has not taken off, i.e. when $z \equiv -L$ (see figure 2).

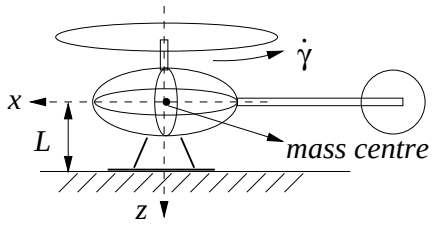

Figure 2: Mass Centre Localization.

Let us choose u in (4) such that:

$$\bar{u} = \bar{M}(\ddot{\eta_d} - \lambda_1\dot{\tilde{\eta}}) + \bar{C}(\dot{\eta_d} - \lambda_1\tilde{\eta}) - \lambda_2(\dot{\tilde{\eta}} + \lambda_1\tilde{\eta}) \quad (7)$$

where $\tilde{\eta} = \eta - \eta_d$, $\eta_d(t) \in C^2(\mathbb{R}^+)$ is a desired trajectory, $\lambda_1 > 0, \lambda_2 > 0$. The input (7) is known to guarantee that $\tilde{\eta}, \dot{\tilde{\eta}}, \ddot{\tilde{\eta}} \to 0$ asymptotically exponentially globally [2].

4.2. Altitude control and take-off.

The basic idea is to use $\dot{\gamma}$ (in fact $\dot{\gamma}_d$) to control the first equation in (1), i.e.

$$c_0\ddot{z} + c_7 = c_8\dot{\gamma}^2 u_1 + c_9\dot{\gamma} + c_{10} \qquad (8)$$

with u_1 given by (7).

Assuming that $\|\tilde{\eta}^{(i)}\| < \varepsilon$, $i = 0, 1, 2$, and $\dot{\phi}_d = 0$ one can approximate u_1 in (7) as

$$u_1^{app} = \frac{1}{a_{31}}[c_5\ddot{\gamma}_d - c_{14}\dot{\gamma_d}^2 - c_{15}] \qquad (9)$$

From (8) and (9) it is clear that if $\dot{\gamma}_d$ is constant, then $z(t) = at^2 + bt + c$, $a, b, c \in \mathbb{R}$. An event-based hybrid control strategy for the choice of $\dot{\gamma}_d$ can be designed to stabilize z and $\dot{z}$ in a neighborhood of desired values $z_d, \dot{z_d}$, or at least to make the helicopter take-off the ground and reach a certain height. Then one may switch the control to some nonlinear input guaranteeing global asymptotic tracking of z, $\dot{z}$ and ϕ, $\dot{\phi}$.

There are several crucial choices in this procedure:

1. The input in (7) to control $S_{rotational}$.
2. $\dot{\gamma}_d(t)$ and the hybrid strategy to control $S_{translational}$.
3. $\eta_d(t)$ to comply with input saturations $u_m^1 \leq u_1 \leq 0$ and $u_m^2 \leq u_2 \leq u_M^2$. Here $u_m^i < 0$, $i = 1, 2$ and $u_M^2 > 0$.
4. The identification of physical parameters c_i in particular the drag coefficient of the main rotor and the slope of the sustentation force curve.

The technique employed to cope with input saturations is as follows: from (7) and assuming perfect tracking ($\tilde{\eta} = \dot{\tilde{\eta}} \equiv 0$) one sets

$$u = \bar{A}^{-1}(\dot{\gamma}_d(t))[\bar{M}(\eta_d)\ddot{\eta}_d + \bar{C}(\eta_d,\dot{\eta}_d)\dot{\eta}_d - \bar{B}(\dot{\gamma}_d)] \qquad (10)$$

From this expression one calculates off-time whether $u_m^1 \leq u_1 \leq 0$ and $u_m^2 \leq u_2 \leq u_M^2$. Then the saturations are respected provided the initial tracking errors $\tilde{\eta}(0)$ and $\dot{\tilde{\eta}}(0)$ and the feedback gains λ_1, λ_2 are chosen small enough. Moreover some numerical results presented below show that the input may saturate during the transient without destroying the stability of the closed-loop system.

When $\ddot{\gamma}_d \equiv 0$, $\dot{\gamma}_d = constant$, a sufficient condition to get a negative u_1 input in (10) is given by

$$c_6 \sin(2c_3\gamma_d)\dot{\phi}_d^2 + c_{14}\dot{\gamma}_d^2 + c_{15} \geq 0 \qquad (11)$$

5. Simulation Results.

We have made some simulation experiments in Matlab/Simulink for the 3-DOF system. Here we

present two of them. For each simulation we have taken the gain values of the control (7) $\lambda_1 = 8$ and $\lambda_2 = 10$. In all cases we used a fixed-step ode4 Runge-Kutta solver with step 0.005. Results concerning the flying mode ($z < -L$) are not presented here but can be easily simulated. The control of the rotational dynamics in (6) is in itself a challenging problem.

5.1. Simulation 1.

This is a regulation problem for the desired values given below with the next initial conditions $\phi_0 = 0\ rad$, $\dot{\phi}_0 = 2\ rad/s$, $\gamma_0 = -5\ rad$ and $\dot{\gamma}_0 = -52\ rad/s$. The helicopter in not taking-off the ground. In a first case the initial error $\dot{\tilde{\gamma}} = 33$, for a second case we have reduced this error to $\dot{\tilde{\gamma}} = 7$

- $\phi_d = -\pi/4\ rad$
- $\dot{\phi}_d = 0\ rad/s$
- $\ddot{\phi}_d = 0\ rad/s^2$
- $\gamma_d = -85t\ rad$
- $\dot{\gamma}_d = -85\ rad/s$
- $\ddot{\gamma}_d = 0\ rad/s^2$

5.2. Simulation 2.

This is a regulation and tracking problem defined below. The helicopter in not taking-off the ground.

- $\phi_d = 10\sin(t/10)\ rad$
- $\dot{\phi}_d = \cos(t/10)\ rad/s$
- $\ddot{\phi}_d = -\frac{1}{10}\sin(t/10)\ rad/s^2$
- $\gamma_d = -75t\ rad$
- $\dot{\gamma}_d = -75\ rad/s$
- $\ddot{\gamma}_d = 0\ rad/s^2$

5.3. Simulation 3.

This set of figures concern the same regulation problem as simulation 1 but with decreased values of λ_1 and λ_2 taken equal to 1 and smaller initial errors.

5.4. Comments.

From figures 3 to 23 the following comments can be made: the tracking and regulation error converge towards zero after a transient period that seems to be more or less independent of the initial error on the rotor speed (compare figures 6 and 7, figures 4 and 8, figures 5 and 9). From figures 10, 13, 22, 23 one sees that the saturation of the inputs during the transient does not destroy the stability of the closed-loop system, although such saturating control is certainly not desirable in practice. The chosen desired angles and velocities satisfy the constraint (11), and the saturations are a consequence of the initial errors and of the feedback gains λ_1 and λ_2. It is known that one drawback of nonlinear controllers as in (7) is that tuning the gains is not an easy task in general [2]. In figures 24 and 29 one sees that decreasing the feedback gains and the initial errors allows one to respect the input saturations and to improve the transient behaviour.

6. Conclusions.

In this note we have considered the feedback control of a scale model helicopter mounted on a platform. The resulting model is a 3-DOF Lagrangian system, with 2 inputs. This is therefore an underactuated system. Some aerodynamical effects have been incorporated in the model to obtain the generalized torques as a function of the inputs (the collective pitch angles of the main and tail rotors) and of the main rotor angular velocity. The complete model also incorporates the transition from the constrained mode (the helicopter is at rest on the ground) to the flying mode (the helicopter is airborne).

The proposed control strategy is based on the use of nonlinear controllers which assure asymptotic tracking of suitable (i.e. differentiable enough and such that the inputs do not saturate) desired trajectories. Mechanical and aerodynamical coupling effects are taken into account in the model and in the control action. The dissipativity properties of the rotational part of the dynamics are used to partially design the state feedback control. Numerical simulations are presented and experiments on a scale model Benzin Trainer are planned.

Future work will focus on the extension of this control strategy to the "free" helicopter (the 7-DOF system), and experimental validation on the scale model helicopter of the University of Technology of Compiègne (France). Robustness of the controllers with respect to neglected dynamics and external disturbances will be tested.

A. Model Parameters.

The values of the constant physical parameters

are given in table 1. We have supposed that the system evolves in standard atmosphere conditions.

c_i	$Value$	c_i	$Value$
c_0	7.5	c_8	0.6251093
c_1	0.436087	c_9	0.1207317
c_2	$1.3872e-4$	c_{10}	3.6787
c_3	-4.1428571	c_{11}	-0.0453127
c_4	$7.35875e-2$	c_{12}	2.1463432
c_5	0.436826	c_{13}	100
c_6	$2.8734857e-4$	c_{14}	$1.9630356e-4$
c_7	-73.575	c_{15}	-0.5181731

Table 1: Physical Parameters.

References

[1] Koo, T. J. and Sastry, S., *Output Tracking Control design of a Helicopter Model Based on Approximate Linearization*, 37th IEEE Conference on Decision and Control, Florida, USA, 1998.

[2] Lozano, R., Brogliato, B., Egeland, O. and Maschke, B., *Dissipative Systems Analysis and Control. Theory and Applications*, Springer Verlag, CCE Series, London, 2000.

[3] Mahony, R. and Lozano, R., *An Energy Based Approach to the Regulation of a Model Helicopter near to Hover*, European Control Conference, Karlsruhe, Germany, September 1999.

[4] Prouty, R. W., *Helicopter Performance, Stability and Control*, Krieger Publishing Company, 1995.

[5] Sira-Ramírez, H., Zribi, M. and Ahmed, S., *Dynamical Sliding Mode Control Approach for vertical Flight Regulation in Helicopters*, IEE Proc.-Control Theory Appl., Vol. 141, No. 1, pp. 19-24, January 1994.

[6] Stepniewsky, W. Z., *Rotor-wing Aerodynamics*, Vol. 1 *Basic Theories of Rotor Aerodynamics*, Dover Publishing., Inc., N. Y., 1984.

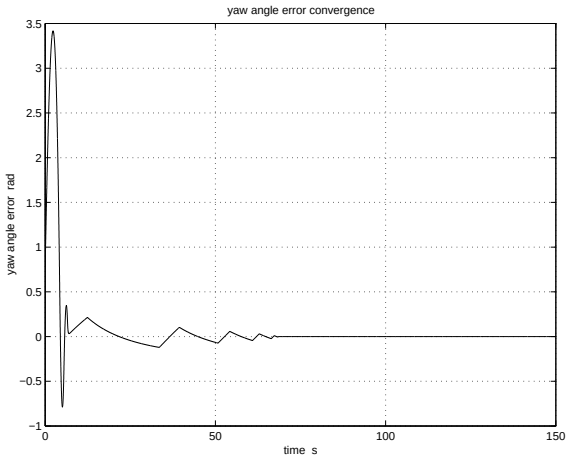

Figure 3: Yaw Angle Error for Simulation 1, $\dot{\tilde{\gamma}}(0) = 32\ rad/s$.

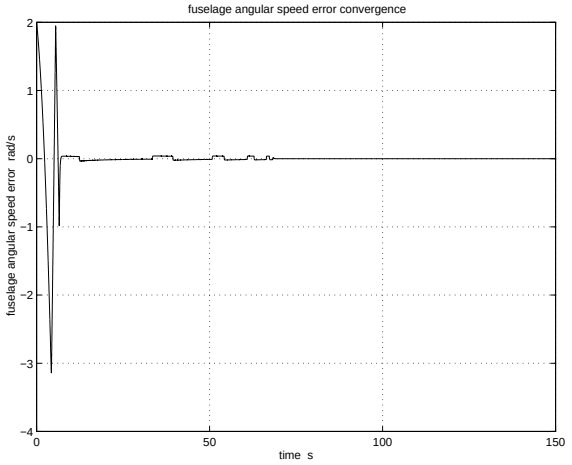

Figure 4: Fuselage Angular Speed Error for Simulation 1, $\dot{\tilde{\gamma}}(0) = 32\ rad/s$.

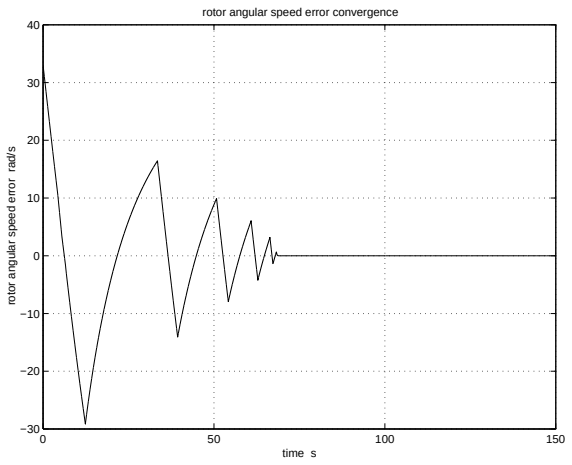

Figure 5: Rotor Angular Speed Error for Simulation 1, $\dot{\tilde{\gamma}}(0) = 32\ rad/s$.

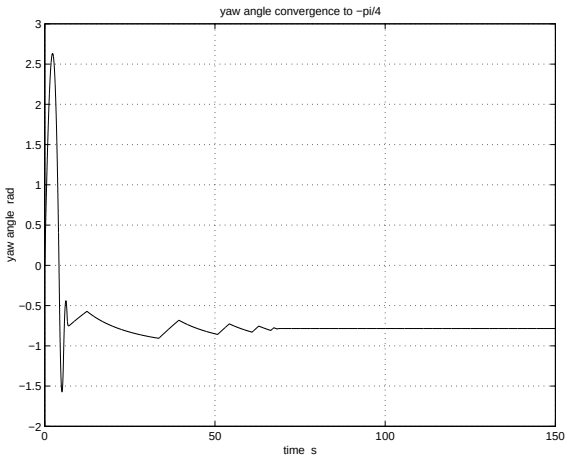

Figure 6: Yaw Angle for Simulation 1, $\dot{\tilde{\gamma}}(0) = 32\ rad/s$.

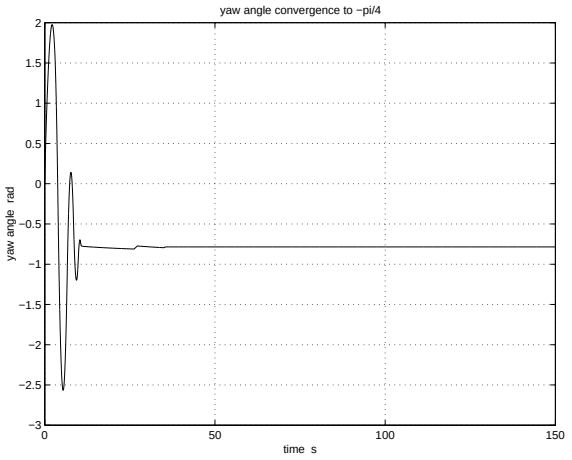

Figure 7: Yaw Angle for Simulation 1, $\dot{\tilde{\gamma}}(0) = 7\ rad/s$.

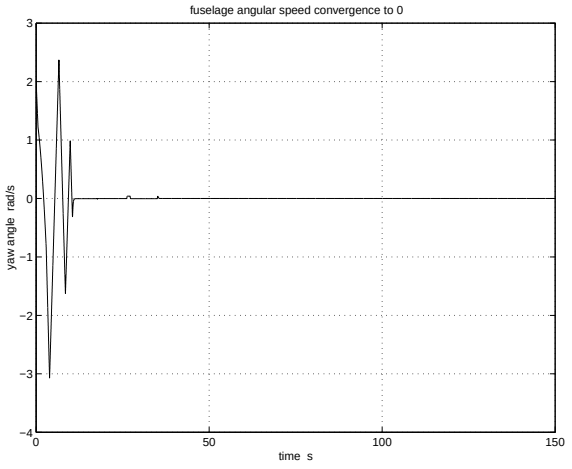

Figure 8: Fuselage Angular Speed for Simulation 1, $\dot{\tilde{\gamma}}(0) = 7\ rad/s$.

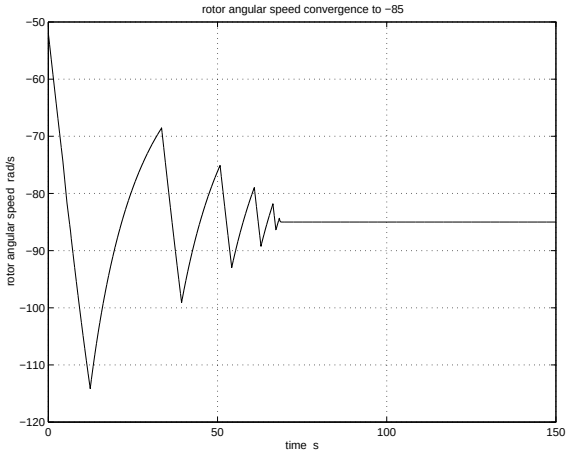

Figure 9: Rotor Angular Speed for Simulation 1, $\dot{\tilde{\gamma}}(0) = 32\ rad/s$.

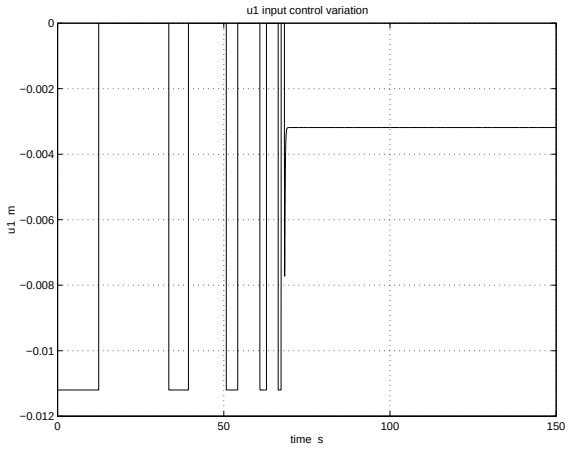

Figure 10: u_1 Input Control for Simulation 1, $\dot{\tilde{\gamma}}(0) = 32\ rad/s$.

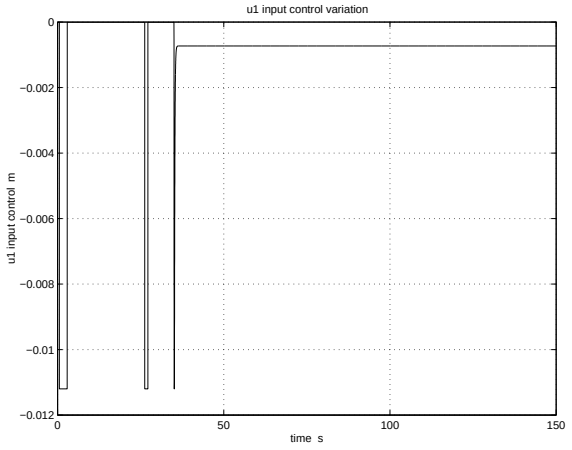

Figure 11: u_1 Input Control for Simulation 1, $\dot{\tilde{\gamma}}(0) = 7\ rad/s$.

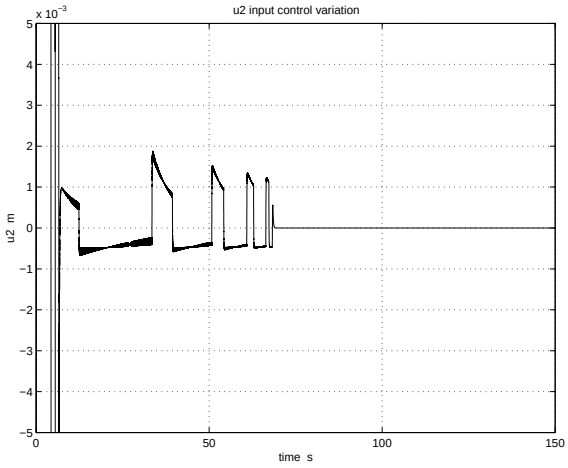

Figure 12: u_2 Input Control for Simulation 1, $\dot{\tilde{\gamma}}(0) = 32\ rad/s$.

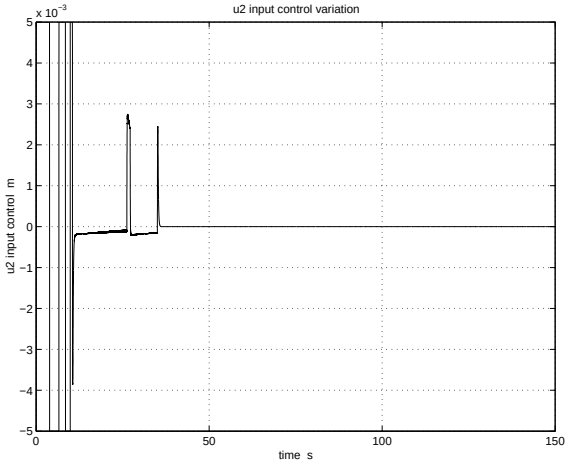

Figure 13: u_2 Input Control for Simulation 1, $\dot{\tilde{\gamma}}(0) = 7\ rad/s$.

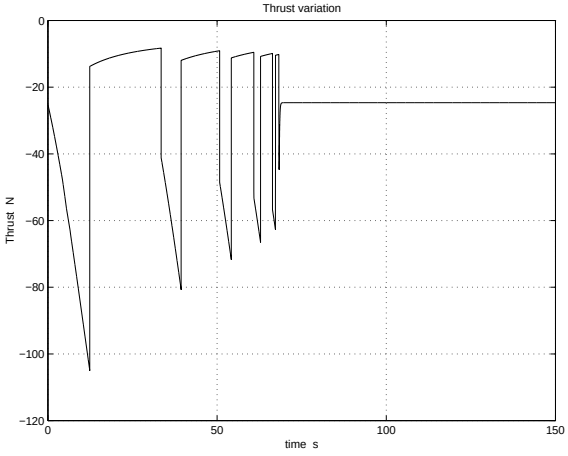

Figure 14: Thrust for Simulation 1, $\dot{\tilde{\gamma}}(0) = 32\ rad/s$.

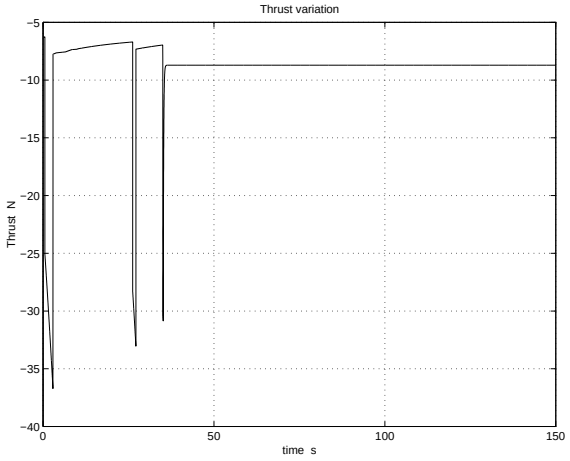

Figure 15: Thrust for Simulation 1, $\dot{\tilde{\gamma}}(0) = 7\ rad/s$.

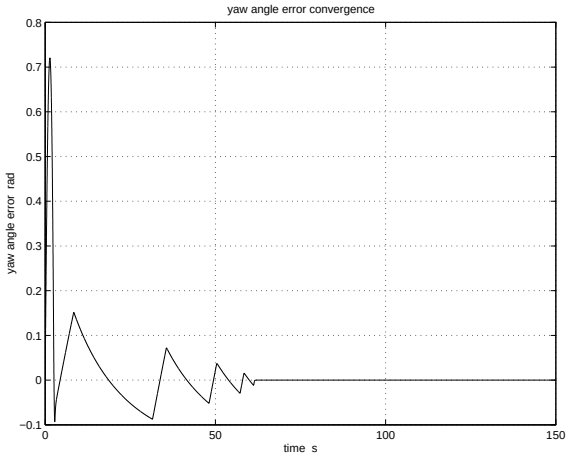

Figure 16: Yaw Angle Error for Simulation 2.

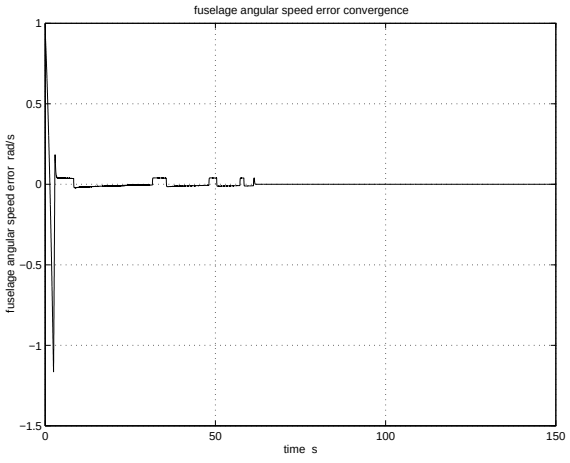

Figure 17: Fuselage Angular Speed Error for Simulation 2.

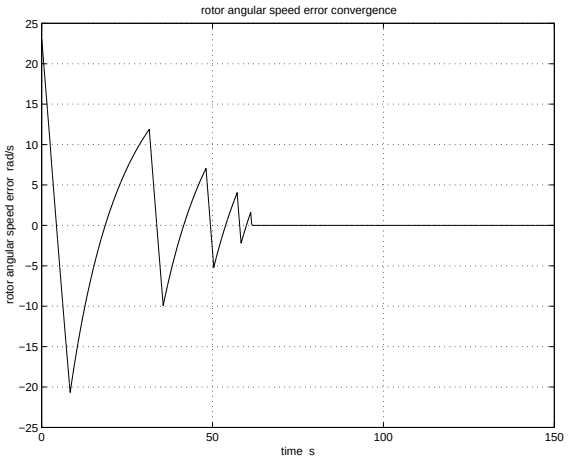

Figure 18: Rotor Angular Speed Error for Simulation 2.

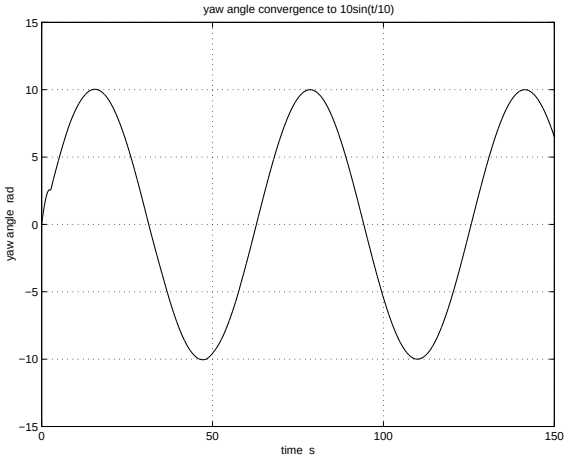

Figure 19: Yaw Angle for Simulation 2.

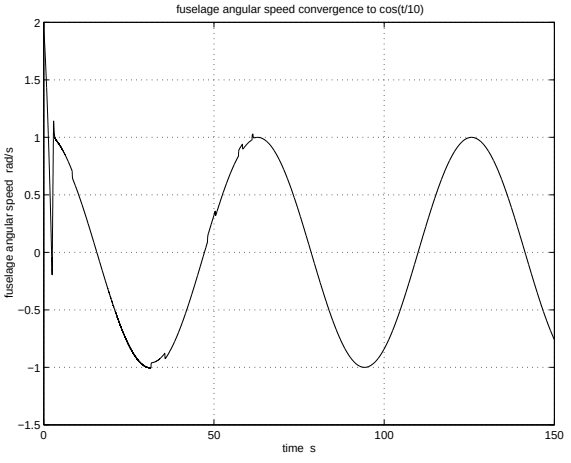

Figure 20: Fuselage Angular Speed for Simulation 2.

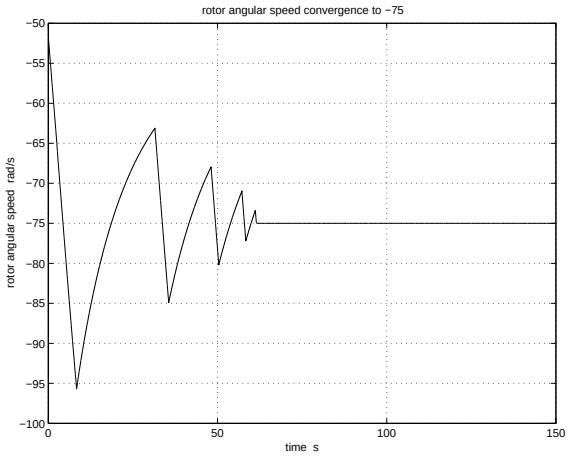

Figure 21: Rotor Angular Speed for Simulation 2.

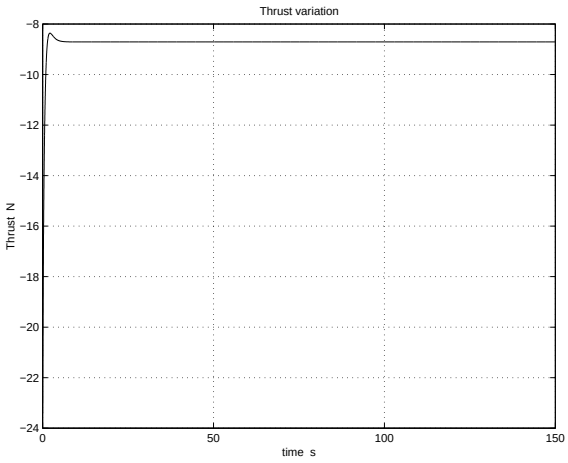

Figure 24: Thrust for Simulation 3.

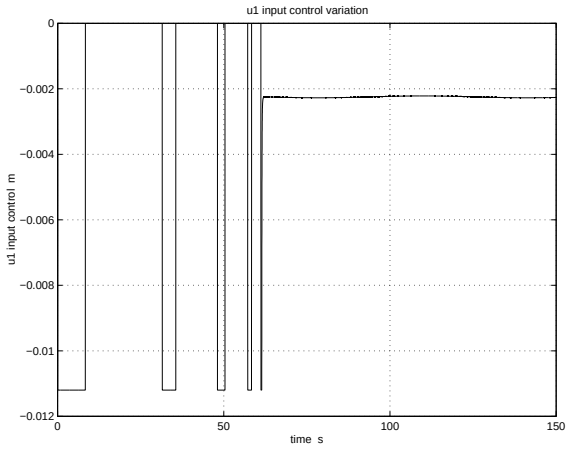

Figure 22: u_1 Input Control for Simulation 2.

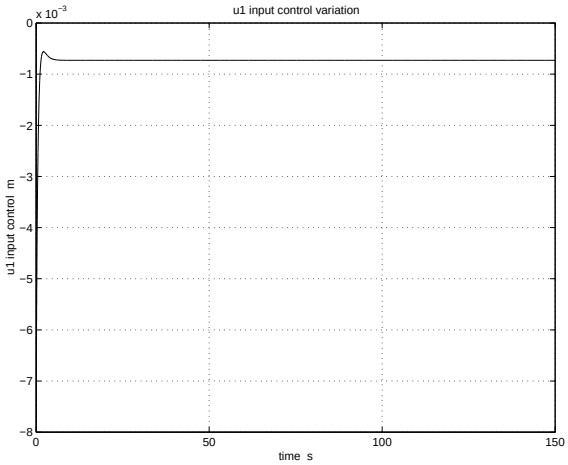

Figure 25: u_1 Input Controlfor Simulation 3.

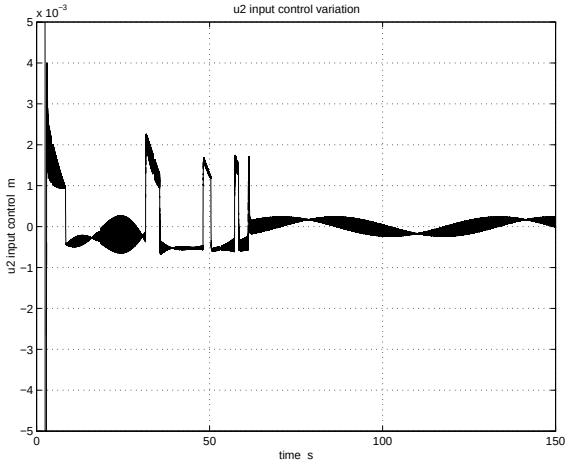

Figure 23: u_2 Input Control for Simulation 2.

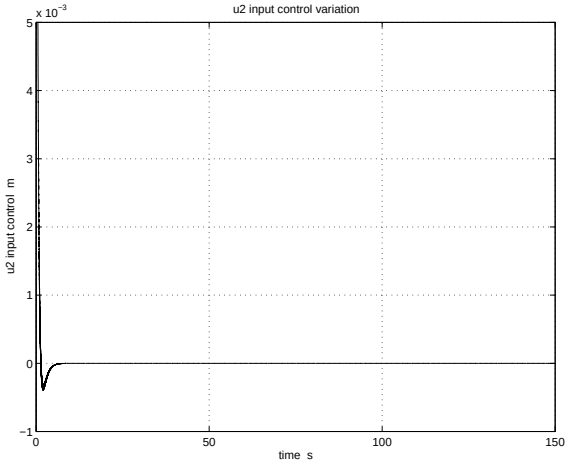

Figure 26: u_2 Input Control for Simulation 3.

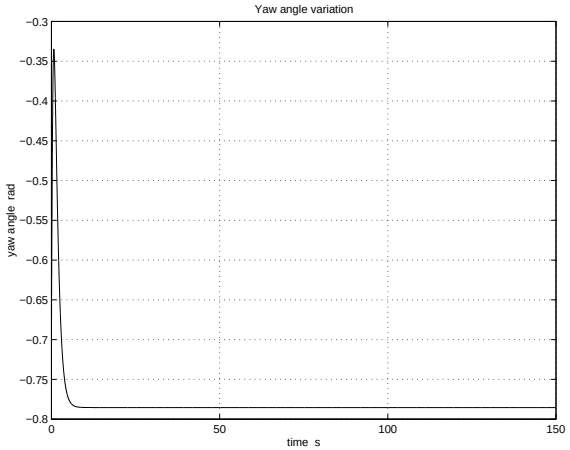

Figure 27: Yaw Angle for Simulation 3.

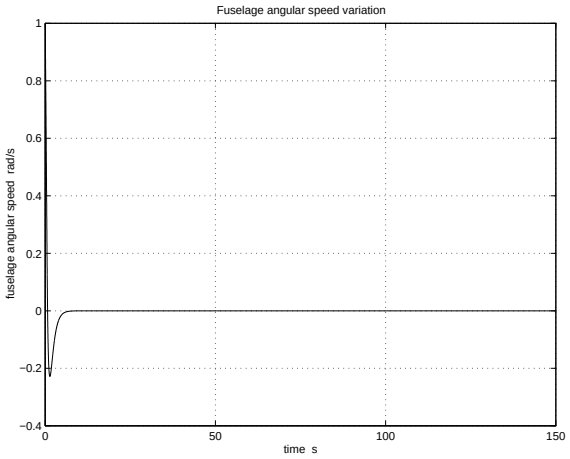

Figure 28: Fuselage Angular Speed for Simulation 3.

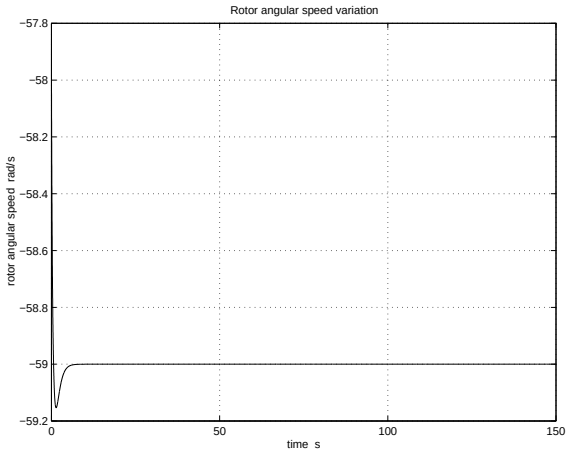

Figure 29: Rotor Angular Speed for Simulation 3.